

Influence of sintering temperatures on the electrical property of bismuth sodium titanate based piezoelectric ceramics

Laijun Liu · Huiqing Fan

© Springer Science + Business Media, LLC 2006

Abstract A systematic investigation of cerium and stannum doped $0.94(\text{Bi}_{0.5}\text{Na}_{0.5})\text{TiO}_3-0.06\text{BaTiO}_3$ (Sn&Ce-BNT6BT) based lead-free piezoelectric ceramics is undertaken to understand the influence of sintering temperature on electrical properties. The X-ray diffraction patterns showed that all of the Sn&Ce-BNT6BT ceramics exhibited a single perovskite structure with the co-existence of the rhombohedral and tetragonal phase. The smaller grain size of Sn&Ce-BNT6BT ceramics was obtained at lower sintering temperature, and more cubical grains of Sn&Ce-BNT6BT ceramics were obtained at higher sintering temperature. The temperature dependence of dielectric permittivity of the compositions exhibited strong dispersion with the increasing temperature, and the dielectric loss tangent increased dramatically while the temperature over 225°C . The depolarization temperature T_d of Sn&Ce-BNT6BT ceramics sintered at 1160°C was 92.6°C . The remnant polarizations P_r for Sn&Ce-BNT6BT ceramics sintered at 1120 and 1200°C were found to be 28.8 and $33.4 \mu\text{C}/\text{cm}^2$ at room temperature, respectively.

Keywords Bismuth sodium titanate · Sintering · Piezoelectric properties

1 Introduction

Bismuth sodium titanate, $(\text{Bi}_{0.5}\text{Na}_{0.5})\text{TiO}_3$ (abbreviated as BNT), is considered to be an excellent candidate for lead-

free piezoelectric ceramics. The BNT ceramics exhibit a large remnant polarization $P_r = 38 \mu\text{C}/\text{cm}^2$, a higher Curie temperature $T_c = 320^\circ\text{C}$ and a phase transition point from ferroelectric to antiferroelectric $T_p = 200^\circ\text{C}$. However, data on piezoelectric properties of the BNT ceramic are scarce because it is difficult to pole this ceramic due to its large coercive field $E_c = 73 \text{ kV}/\text{cm}$ [1–3]. Therefore, BNT-based solid solutions have recently been studied to improve their poling behavior. Particularly, a large piezoelectricity is expected for the BNT-based solid solutions with a morphotropic phase boundary (MPB). Among BNT-based systems, $(1-x)[(\text{Bi}_{0.5}\text{Na}_{0.5})\text{TiO}_3]-x\text{BaTiO}_3$ (BNTBT) is more interesting. The morphotropic phase boundary (MPB) composition is at $x = 0.06$, where the ceramic presents relatively marked piezoelectric properties [4].

It is well known that CeO_2 is a commonly used additive for lead base $\text{Pb}(\text{Zr},\text{Ti})\text{O}_3$ ceramics. It can generally show the interesting effects on improving the piezoelectric properties of $\text{Pb}(\text{Zr},\text{Ti})\text{O}_3$ ceramics and decreasing the dissipation factor at the same time. The mechanism for the effect of CeO_2 is very complicate. The result may concern with their simultaneous effect as its effect on $\text{Pb}(\text{Zr},\text{Ti})\text{O}_3$ ceramics [5]. In our previous work, we found that small amounts of dopants like CeO_2 and SnO_2 had dramatic effects on dielectric and piezoelectric properties of BNT ceramics.

However, most properties of piezoelectric ceramics, like density, dielectric and piezoelectric properties, strongly depend on the sintering temperature. Therefore, it is necessary to investigate the effect of sintering temperatures on the structure and properties of BNT-based piezoelectric ceramics. In this work, dielectric and piezoelectric properties at room temperature of $0.4 \text{ wt}\%$ Sn and $0.4 \text{ wt}\%$ Ce doped $0.94 (\text{Bi}_{0.5}\text{Na}_{0.5})\text{TiO}_3-0.06\text{BaTiO}_3$ (Sn&Ce-BNT6BT) component sintered at different temperatures are studied carefully.

L. Liu · H. Fan (✉)
State Key Laboratory of Solidification Processing,
School of Materials Science and Engineering, Northwestern
Polytechnical University,
Xi'an 710072, China
e-mail: hqfan3@163.com

2 Experimental

The Sn&Ce-BNT6BT ceramics were prepared by a solid sintering technique. Reagent-grade oxide or carbonate powders of Bi_2O_3 , Na_2CO_3 , BaCO_3 , TiO_2 , SnO_2 and CeO_2 were used as the starting materials. The powders of these raw materials were mixed by a vibrating mill with hard steel ball for 6h and calcined at 900°C for 1.5 h. After calcining, the powders were mixed by the vibrating mill with iron ball for 6 hours again, then added into 25 wt% binder and rolled into square platelet of $12 \times 12 \times 0.5$ mm. After removing binder, the platelets were sintered at 1120 – 1200°C for 1 h in the air atmosphere.

The surface morphologies of the sintered specimens were observed by a scanning electron microscope (SEM; JSM-5610, JEOL, Tokyo, Japan). The grain size was obtained using a line intercept method. X-ray diffraction patterns were obtained using an automated diffractometer (XRD; X'Pert PRO MPD, Philips, Eindhoven, Netherlands) with $\text{Cu K}\alpha$ radiation. Fired-on silver paste was used for the electrodes for the dielectric and piezoelectric measurements. Specimens for piezoelectric measurements were poled at 160 – 170°C in a silicone oil bath by applying a DC electric field of 3–4 kV/mm for 20 min. The piezoelectric coefficient (d_{33}) was measured using a piezoelectric d_{33} -meter (ZJ-4NA, Institute of Acoustics Academic Sinica, Beijing, China) at a frequency of 100 Hz. The electromechanical coupling factors (k_p , k_t) and the mechanical quality factor (Q_m) were measured by the resonance and anti-resonance technique using an impedance analyzer (4294A, Agilent, Palo Alto, CA, USA) [6].

3 Results and discussion

Figure 1 shows X-ray powder diffraction patterns for Sn&Ce-BNT6BT sintered at 1120°C , 1140°C , 1160°C , 1180°C and

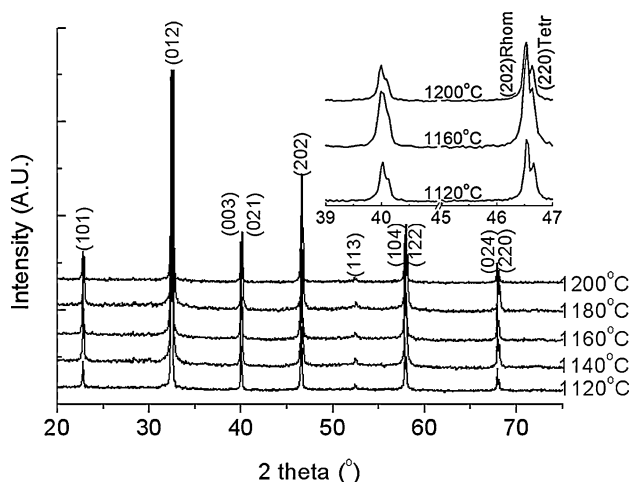


Fig. 1 XRD patterns of Sn&Ce-BNT6BT ceramics sintered at different temperatures, inset, XRD analysis in the 2θ ranges 39 – 41° and 45 – 47°

1200°C , respectively. These patterns show a single phase of perovskite structure sintered at different temperatures. The further XRD analysis performed in the 2θ ranges 39 – 41° and 45 – 47° is shown in the inset. At room temperature, the $\text{Bi}_{0.5}\text{Na}_{0.5}\text{TiO}_3$ system is in rhombohedral phase and BaTiO_3 is in tetragonal phase. There is a rhombohedral–tetragonal MPB in their solid solution near $0.94(\text{Na}_{0.5}\text{Bi}_{0.5})\text{TiO}_3$ – 0.06BaTiO_3 composition [4]. X-ray diffraction pattern of the composition at MPB is characterized with separated presence of two peaks to (003)/(021) at about 39.88° and splitting of the peak to (202) planes at around 46.58° [7]. In the inset, X-ray pattern exhibits the feature of peak splits at corresponding diffraction angles, indicating co-existence of tetragonal and rhombohedral phases in Sn&Ce-BNT6BT sample.

Figure 2 shows the SEM micrographs of Sn&Ce-BNT6BT sintered at different temperatures on the surface of the bulk. There are two kinds of grains that exist mainly on the ceramic surface: spherical and cubical shape. The spherical grains range in diameter from 0.4 to $2 \mu\text{m}$, and the cubical grains range in diameter from 2 to $3.5 \mu\text{m}$ (Table 1). It is evident that smaller grain sizes of Sn&Ce-BNT6BT ceramics appear at lower sintering temperatures, and more cubical grains of Sn&Ce-BNT6BT ceramics are obtained at middle temperatures. As the sintering temperature increases, the grain size also increases dramatically.

Figure 3 shows the permittivity ϵ_r and dielectric loss tangent $\text{Tan}\delta$, as a function of temperature for Sn&Ce-BNT6BT ceramics sintered at 1160°C . The permittivity–temperature curves of the composition exhibit strong dielectric dispersion with the increasing temperature. This phenomenon could be a result of the diffuse phase transition, because BNTBT system is a typical relaxation ferroelectric with A-site complex ions [8]. As shown in Fig. 3, for the BNT6BT doped Ce^{4+} and Sn^{4+} , there is a sharp increase in permittivity near 100°C . After that, the argument of the increase becomes slow and the curve begins to broaden. This inflexion was called “a shoulder” on the curve in some reports and indicated an intermediate phase transition [9]. An opinion about this shoulder is that the temperature region between the shoulder and T_{max} (here “ T_{max} ” is the temperature at which ϵ has the maximum value) is an anti-ferroelectric phase [9]. A similar phenomenon was found in PLZT ceramics and the respondent explanation was a macro–micro domain switching [10, 11]. Here, the temperature where the transition between ferroelectric phase and anti-ferroelectric phase is called as depolarization temperature (T_d), the T_d of Sn&Ce-BNT6BT ceramics sintered at 1160°C is 92.6°C . In general the dielectric loss tangent for this composition decreases with increasing frequency and shows no significant anomaly near transition temperature as observed from the temperature dependent permittivity measurement. The dielectric loss tangent increases with the increase of sintering temperature particularly beyond 225°C . The increase in dielectric loss tangent at higher temperature

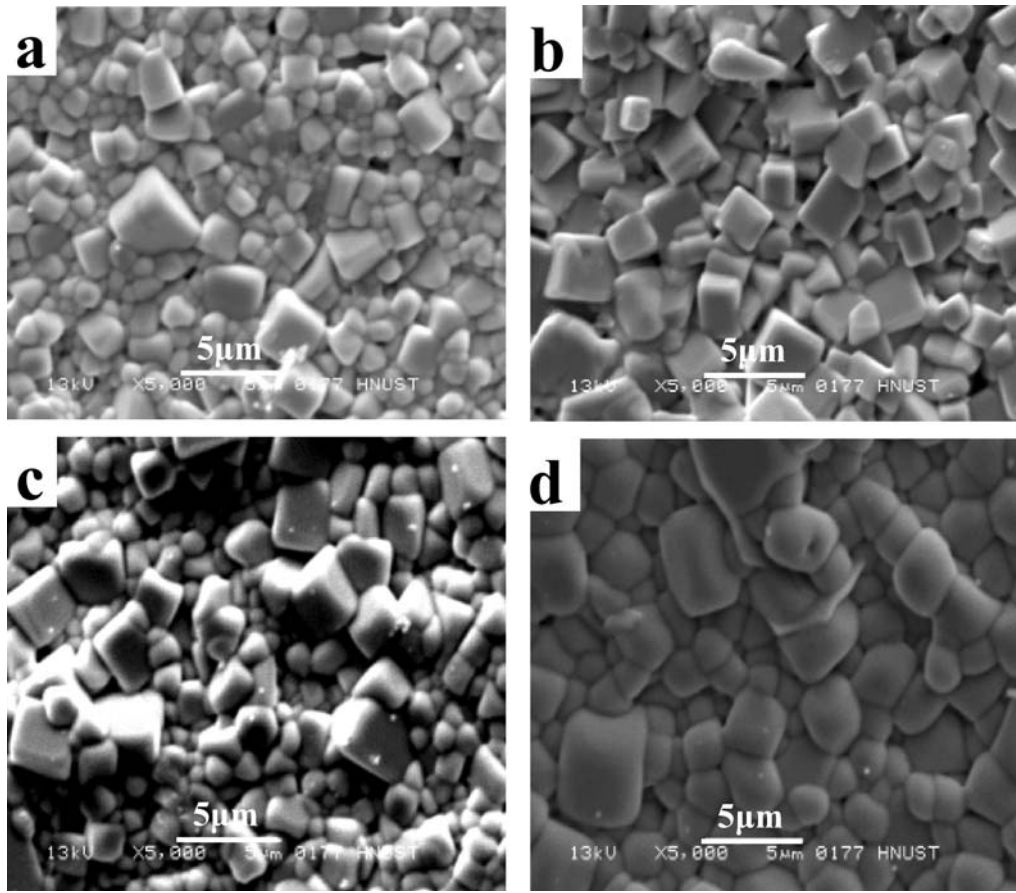


Fig. 2 SEM micrographs of the surface Sn&Ce-BNT6BT ceramics sintered at different temperatures: (a) 1120°C, (b) 1140°C, (c) 1160°C, (d) 1180°C

might be due to the formation of higher concentration of charge carriers.

Figure 4 shows the P – E hysteresis loops of Sn&Ce-BNT6BT ceramics sintered at 1120°C and 1200°C obtained at room temperature. Remnant polarizations P_r at room temperature are found to be about 28.8 and 33.4 $\mu\text{C}/\text{cm}^2$ for the systems sintered at 1120 and 1200°C, respectively, which are higher than the values in earlier reports on the BNT-BT system. The increase in P_r in the system can be attributed to the increase in the MPB nature of the system due to dipole moments of the samples close to the MPB being able to

reorientate themselves more completely after the Ce^{4+} and Sn^{4+} entering into the crystal lattice. The P_r increase can also be associated with the increase in domain wall motion that switches domains and hence affects the polarization. It can be seen that the squareness of the P – E loops increases with increasing sintering temperature from the figure, which suggests the increment of long-range co-operation between dipoles with the increase of temperature.

The detailed dielectric and electromechanical properties of Sn&Ce-BNT6BT ceramics sintered at different temperatures are shown in Table 1. The Sn&Ce-BNT6BT ceramics

Table 1 Grain size and dielectric, piezoelectric and mechanical properties of Sn&Ce-BNT6BT ceramics sintered at different temperatures

Sintering temperature	1120°C	1140°C	1160°C	1180°C	1200°C
Grain size (μm)	0.8–2.5	0.6–2.5	0.6–2.7	0.7–2.9	1.3–3.4
Loss tangent, $\tan\delta$	0.025	0.020	0.020	0.018	0.020
Dielectric permittivity, ϵ_r	898	1103	989	1073	859
Thick coupling factor, k_t	0.46	0.37	0.38	0.37	0.44
Planar coupling factor, k_p	0.20	0.16	0.22	0.18	0.19
The ratio of k_t/k_p	2.3	2.2	1.7	1.8	1.8
Mechanical quality factor, Q_m	158	121	104	185	180
Frequency constant, Np (Hz·m)	2410	2514	2573	2635	2278
Piezoelectric coefficient, d_{33} (pC/N)	63	79	92	83	81

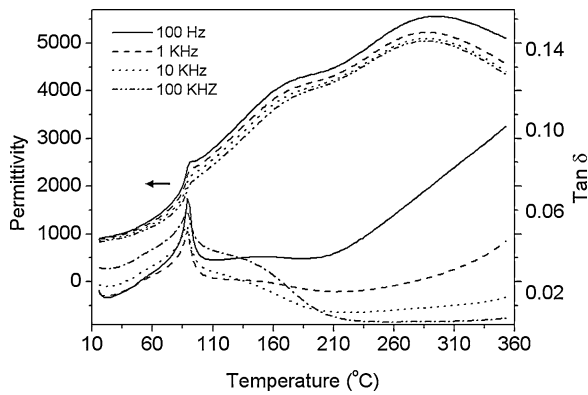


Fig. 3 Temperature dependence of dielectric permittivity and dielectric loss of Sn&Ce-BNT6BT ceramics sintered at 1160°C

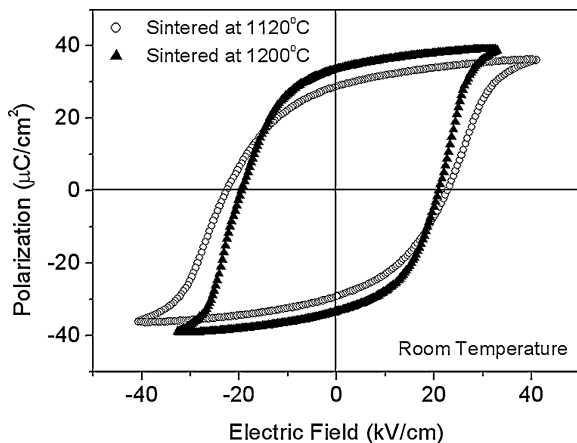


Fig. 4 P - E hysteresis loops of Sn&Ce-BNT6BT ceramics sintered at 1120°C and 1200°C, respectively

sintered at different temperatures all have applicable electrical properties. From the Table 1, the relative dielectric permittivity ϵ_r (1 kHz) and the dielectric loss tangent $\tan\delta$ (1 kHz) do not appear to change with a continuous increasing sintering temperature, is about 1000 and 0.02 at room temperature, respectively. The planar electric-mechanical coupling factor k_p changes little when the sintering temperature is over 1160°C, but the k_p value is larger than that of ceramics sintered at 1140°C. The rule of change for the thick electric-mechanical coupling factor k_t is difficult to illuminate, but the larger k_t value is obtained when the Sn&Ce-BNT6BT ceramics are sintered at 1140°C and 1200°C. The ratio of k_t/k_p is an important parameter for ultrasonic transducers, the k_t/k_p of the Sn&Ce-BNT6BT ceramics ranges from 1.7 to 2.3 while the sintering temperature changes from 1120°C to 1200°C, which can satisfy well applied requirement. As the sintering temperature increases, the mechanical quality factor, Q_m decreases when the sintering temperature is below 1160°C, then reaches a peak at 1180°C. The maximum of mechanical quality factor $Q_m = 185$ is obtained when the ceramics are sintered at 1180°C for one hour. The piezoelectric coefficient, d_{33} increases when the temperature

is below 1160°C, then decreases at a higher temperature. The maximum $d_{33} = 92\text{pC/N}$ is obtained at 1160°C. These characters make Sn&Ce-BNT6BT suitable for narrowband filters and ultrasonic transducers.

4 Conclusions

The phase structure, microstructure, piezoelectric and dielectric properties of Sn&Ce-BNT6BT ceramics are investigated deeply. All of the Sn&Ce-BNT6BT ceramics sintered at different temperatures exhibited a single perovskite structure with the co-existence of the rhombohedral and tetragonal phase. The temperature dependence of permittivity of the compositions exhibited strong dielectric dispersion with the increasing temperature. The dielectric loss tangent increased while the temperatures were beyond 225°C. The depolarization temperature T_d of Sn&Ce-BNT6BT ceramics sintered at 1160°C was 92.6°C, which did not change remarkably as sintering temperature increased. Remnant polarizations P_r at room temperature obtained were about 28.8 and 33.4 $\mu\text{C}/\text{cm}^2$ for the systems sintered at 1120 and 1200°C, respectively. The remnant polarization P_r for this system at room temperature increased with increase the sintering temperature.

Acknowledgments National Nature Science Foundation and Nature Science Foundation of Shaanxi Province and the Excellent Young Teachers Program of MOE and Science Creative Foundation and Graduate Starting Seed Foundation of NPU of China have supported this work.

References

- G.A. Smolenskii, V.A. Isupov, A.I. Agranovskaya, and N.N. Krainik, *Sov. Phys.-Solid State (Engl. Transl.)*, **2**(11), 2651 (1961).
- J. Suchanicz, K. Roleder, A. Kania, and J. Handerek, *Ferroelectrics*, **77**, 107 (1988).
- M.S. Hagiyeve, I.H. Ismaizade, and A.K. Abiyev, *Ferroelectrics*, **56**, 215 (1984).
- T. Takenaka, K. Maruyama, and K. Sakata: *Jpn. J. Appl. Phys.*, **30**, 2236 (1991).
- Y.H. Xu, *Ferroelectric and Piezoelectric Materials* (Science Publishers, Beijing, China, 1978), 161.
- "IEEE Standard on Piezoelectricity", IEEE Standard 176-1978, *Institute of Electrical and Electronic Engineers*, New York (1978).
- M. Onoe, and H. Jumonji. *J. Acoust. Soc. Am.*, **41**(4) 74 (1967).
- T. Takenaka, K.-I. Maruyama, and K. Sakata, *Jpn. J. Appl. Phys.*, **30**(9B) 2246 (1991).
- K. Sakata, T. Takenaka, and Y. Naitou, *Ferroelectrics*, **131**, 219 (1992).
- X. Dai, A. DiGiovanni, and D. Viehland, *J. Appl. Phys.*, **74**(5) 3399 (1993).
- Y. Xi, C. Zhili, and L.E. Cross, *J. Appl. Phys.*, **54**, 3399 (1983).